Segmentation of synthetic aperture radar image using multiscale information measure-based spectral clustering

Haixia Xu (徐海霞)[1], Zheng Tian (田 铮)[2,3], and Mingtao Ding (丁明涛)[2]

[1]*School of Computer Science, Northwestern Polytechnical University, Xi'an 710072*

[2]*School of Science, Northwestern Ploytechnical University, Xi'an 710072*

[3]*State Key Laboratory of Remote Sensing Science, Institute of Remote Sensing Applications, Chinese Academy of Sciences, Beijing 100101*

Received June 22, 2007

A multiscale information measure (MIM), calculable from per-pixel wavelet coefficients, but relying on global statistics of synthetic aperture radar (SAR) image, is proposed. It fully exploits the variations in speckle pattern when the image resolution varies from course to fine, thus it can capture the intrinsic texture of the scene backscatter and the texture due to speckle simultaneously. Graph spectral segmentation methods based on MIM and the usual similarity measure are carried out on two real SAR images. Experimental results show that MIM can characterize texture information of SAR image more effectively than the commonly used similarity measure.

OCIS codes: 100.0100, 280.0280, 280.6730.

Over the past few years, the development of synthetic aperture radar (SAR) imaging for applications from remote sensing to surface surveillance has experienced a rapid growth. For such applications, segmentation plays a key role in the subsequent analysis for target detection, recognition, and image compression. However, automatic segmentation of SAR image is extremely difficult because of the speckle noise[1]. Although speckle is an intrinsic nature of coherent imaging systems, it is not truly a noise in the typical engineering sense. Ulaby *et al.* have pointed out that texture in SAR image is a combination of intrinsic texture of the scene backscatter and texture due to speckle[2]. Thus, in order to get an accurate segmentation result of SAR image, it appears sensible to give an appropriate texture measure that adapts to the peculiarity of SAR image. Due to the interference among radar returns, the physical attributes of the different classes of terrain give rise to distinct multiscale behavior. For example, grass terrain is composed of many small scatterers while forest terrain is composed of fewer larger scatterers. One would thus expect that there is more correlation between pixels at different scales in the forest case since fewer random variables are involved[3]. To capture the behavior among the different scales of the SAR image, we employ the wavelet transform theory.

Recently, spectral clustering has emerged in the context of segmentation and clustering[4,5]. It does not need the parametric assumptions about data distributions. In addition, it is simple to implement, and can be solved efficiently by standard linear algebra software, and it often outperforms traditional clustering algorithms. It is often described in graph theoretic terms[6]. Let $G(\mathbf{V}, \mathbf{E})$ be an undirected graph with vertex set $\mathbf{V} = \{v_1, \cdots, v_n\}$ and edge set $\mathbf{E} = \{e_{ij}, i, j = 1, \cdots, n\}$. The weight on each edge, w_{ij}, is a function of the similarity between vertices v_i and v_j. The weight matrix of the graph is $\mathbf{W} = \{w_{ij}, i, j = 1, \cdots, n\}$. Define the degree of a vertex v_i as $d_i = \sum_{j=1}^{n} w_{ij}$, the degree matrix $\mathbf{D}$ is the diagonal matrix with the degrees $d_1, \cdots, d_n$ on the diagonal. The spectral clustering method uses the eigenvectors corresponding to certain eigenvalues (the spectrum) of a suitably chosen matrix, usually the weight matrix or the closely related Laplacian matrix, to partition the data. A graph G can be bi-partitioned into two disjoint subsets $\mathbf{C}_1$ and $\mathbf{C}_2$ simply by removing edges between the two parts. The degree of similarity between these two pieces can be computed as a total weight of the edges that have been removed. This quantity is called the Cut:

$$\mathrm{Cut}(\mathbf{C}_1, \mathbf{C}_2) = \sum_{i,j=1}^{N_1,N_2} w_{ij}, \tag{1}$$

where the index $i = 1, \cdots, N_1$ runs over the N_1 vertices of set $\mathbf{C}_1$ and the index $j = 1, \cdots, N_2$ runs over the N_2 vertices of set $\mathbf{C}_2$. The minimum cut criterion given by Wu and Leahy[7] has been used in spectral clustering in Ref. [8]. However, the cut cost favors cutting small sets of isolated vertices in the graph. To compensate for this effect, a number of rather heuristically motivated improvements to the cut cost have been proposed, such as the normalized cut[4], the min-max cut[9], and the foreground cut[10].

Despite that spectral clustering method has been observed to work well in a number of cases, there exist situations when it does not perform very well. The poor results are mainly due to the choice of the weight matrix. In the literatures, it often depends on user-specified parameters. Automatic procedures for proper selection of the similarity measure are rarely discussed.

In order to apply the spectral clustering method to the segmentation of SAR image, the construction of an appropriate similarity measure is very crucial. Thus, we introduce a data-driven information theoretic similarity measure, which can capture the rich statistical information in speckle, to spectral segmentation of SAR image. The rationale is that spatial heterogeneity is regarded as uncertainty, i.e., unpredictability of a sample feature.

1671-7694/2008/040248-03

Thus, such an uncertainty can be measured by resorting to information theory in a mathematically rigorous and physically consistent manner. A suitable criterion is mutual information (MI). In principle, MI measures nonlinear dependencies between a set of random variables taking into account higher order statistical structures existing in the data, as opposed to linear and second-order statistical measures such as correlation and covariance. Suppose that X and Y are two random variables with a joint density function $f_{X,Y}$ and marginal density functions f_X and f_Y. The MI is defined as[11]

$$\mathrm{MI}\left(X,Y\right)=\sum_{x,y}f_{X,Y}\left(x,y\right)\log\frac{f_{X,Y}\left(x,y\right)}{f_X\left(x\right)f_Y\left(y\right)}. \tag{2}$$

Based on MI, we consider the variations in speckle pattern as image resolution varies from course to fine, and apply discrete wavelet transformation (DWT) to the SAR image to be segmented. Here, we exploit the Haar wavelet for simplicity and leave the selection of wavelet as the subject of our future research. At any decomposition level $l=1,\cdots,L$, the input image is transformed into four subbands: LL_l, LH_l, HL_l, and HH_l. LL_l contains the low-frequency portion of the original image, whereas LH_l, HL_l, and HH_l capture the horizontal, vertical and diagonal features in the image, respectively. Thus, for every pixel x in the original image, there are three vectors corresponding to it, i.e. $\{x_{\mathrm{LH}_1},\cdots,x_{\mathrm{LH}_L}\}$, $\{x_{\mathrm{HL}_1},\cdots,x_{\mathrm{HL}_L}\}$, and $\{x_{\mathrm{HH}_1},\cdots,x_{\mathrm{HH}_L}\}$. Then each vector can be modeled as a random variable by defining an appropriate probability distribution. We first assume that the distributions are defined by $\mathbf{P}_{\mathrm{LH}}=\{p_{\mathrm{LH}_l}\}_{l=1}^{L}$, $\mathbf{P}_{\mathrm{HL}}=\{p_{\mathrm{HL}_l}\}_{l=1}^{L}$, and $\mathbf{P}_{\mathrm{HH}}=\{p_{\mathrm{HH}_l}\}_{l=1}^{L}$. For further study on how to use concepts arising from information theory to capture correlation between two pixels in SAR image, assume that there is another pixel y with the probability distributions given by $\mathbf{Q}_{\mathrm{LH}}=\{q_{\mathrm{LH}_l}\}_{l=1}^{L}$, $\mathbf{Q}_{\mathrm{HL}}=\{q_{\mathrm{HL}_l}\}_{l=1}^{L}$, and $\mathbf{Q}_{\mathrm{HH}}=\{q_{\mathrm{HH}_l}\}_{l=1}^{L}$. Using $\{\mathbf{P}_{\mathrm{LH}},\mathbf{P}_{\mathrm{HL}},\mathbf{P}_{\mathrm{HH}}\}$ and $\{\mathbf{Q}_{\mathrm{LH}},\mathbf{Q}_{\mathrm{HL}},\mathbf{Q}_{\mathrm{HH}}\}$, we define the multiscale information measure (MIM) for pixel pair (x,y) in the SAR image as

$$\mathrm{MIM}\left(x,y\right)=\sum_{D}\sum_{l=1}^{L}f_{D_l}\left(x_{D_l},y_{D_l}\right)\times\log\frac{f_{D_l}\left(x_{D_l},y_{D_l}\right)}{p_{D_l}\left(x_{D_l}\right)q_{D_l}\left(y_{D_l}\right)}, \tag{3}$$

where f_{D_l} is the joint density function, D refers to the three spatial orientations. The MIM defined by Eq. (3) can be used to measure the similarity between two pixels x and y. To calculate the MIM, we resort to a concept known as joint histogram, which is given as

$$\mathbf{h}=\begin{bmatrix} h\left(0,0\right) & h\left(0,1\right) & \cdots & h\left(0,M-1\right)\\ h\left(1,0\right) & h\left(1,1\right) & \cdots & h\left(1,M-1\right)\\ \cdots & \cdots & & \cdots\\ h\left(M-1,0\right) & h\left(M-1,1\right) & \cdots & h\left(M-1,M-1\right)\end{bmatrix},$$

but here it is calculated with respect to two pixels in the same image. Let x and y be two pixels in the original image, then the value $h\left(x,y\right)$ $(x,y\in[0,M-1])$ is the number of pixel pairs having the intensity value x in the first pixel and y in the second pixel. M is the number of gray levels used in the image. Through the joint histogram, the probability distributions used in Eq. (3) can be calculated as

$$f_{D_l}\left(x_{D_l},y_{D_l}\right)=\frac{h\left(x_{D_l},y_{D_l}\right)}{\sum\limits_{x_{D_l},y_{D_l}}h\left(x_{D_l},y_{D_l}\right)}, \tag{4}$$

$$p_{D_l}\left(x_{D_l}\right)=\sum_{y_{D_l}}f_{D_l}\left(x_{D_l},y_{D_l}\right), \tag{5}$$

$$q_{D_l}\left(y_{D_l}\right)=\sum_{x_{D_l}}f_{D_l}\left(x_{D_l},y_{D_l}\right). \tag{6}$$

It can be seen from Eqs. (4) – (6) that the joint histogram is the only requirement to determine the weight matrix of SAR image. We use the nearest neighbor interpolation method[12] to estimate the joint histogram of SAR image, in consideration of reducing the computational complexity. Of course, there exist other interpolation algorithms such as linear interpolation[13], cubic convolution interpolation[14], partial volume interpolation[15], and generalized partial volume interpolation[16].

In the following, we choose two real SAR images of 128×128 pixels and demonstrate that the MIM is an appropriate similarity measure for spectral segmentation of SAR image. In order to give comparable results, we put forth first the generally used similarity measure as[4]

$$w_{xy}=\exp\left\{\frac{-\left\|F\left(x\right)-F\left(y\right)\right\|_2^2}{\sigma_I}\right\} *\begin{cases}\exp\left\{\frac{-\|P(x)-P(y)\|_2^2}{\sigma_P}\right\} & \text{if } \left\|P\left(x\right)-P\left(y\right)\right\|_2<r\\ 0 & \text{otherwise}\end{cases}, \tag{7}$$

where $F\left(\cdot\right)$ and $P\left(\cdot\right)$ are gray level and spatial position of pixels x and y, the scaling parameters σ_I and σ_P control how rapidly the similarity falls off with the gray difference and distance between two pixels. They are somewhat sensitive parameters that are usually chosen empirically. Note that $w_{xy}=0$ for any pair of x and y that are more than r pixels apart.

Then, we give the spectral segmentation algorithm described in Ref. [4] as follows.

1) Given an image, set up a weighted undirected graph $G\left(\mathbf{V},\mathbf{E}\right)$ and set the weight on the edge connecting two pixels to be a measure of the similarity between them.

2) Solve the generalized eigenproblem $\left(\mathbf{D}-\mathbf{W}\right)z=\lambda\mathbf{D}z$ for eigenvector $z^{(2)}$ corresponding to the second smallest eigenvalue λ_2.

3) Bipartition the graph G by using $z^{(2)}$.

4) Decide if the current partition should be subdivided and recursively repartition the sub-graph if necessary.

Figure 1 shows the segmentation results using the algorithms based on MIM and common similarity measure.

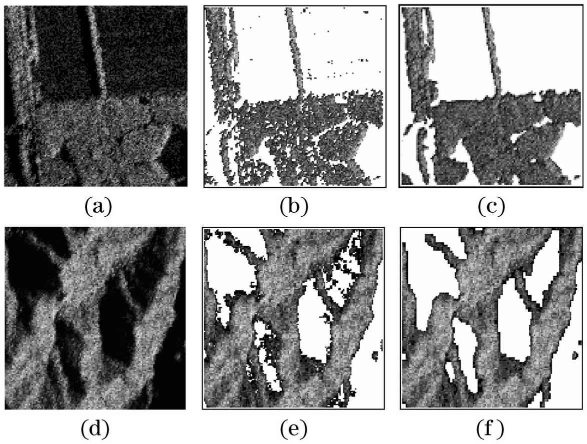

Fig. 1. (a,d) Original SAR images; (b,e) spectral segmentation results based on similarity measure defined by Eq. (7); (c,f) spectral segmentation results based on MIM.

It can be seen that the graph spectral segmentation algorithm based on MIM is robust to the speckle noise and outperforms the algorithm based on common similarity measure.

In conclusion, we define a theoretical concept, MIM, to the spectral segmentation of SAR image. The method takes advantage of multiscale stochastic structure and global statistics information of SAR image. Experimental results confirm that the MIM for spectral segmentation of SAR image is very encouraging.

This work was supported by the National Natural Science Foundation of China (No. 60375003) and the Aeronautics and Astronautics Basal Science Foundation of China (No. 03I53059). H. Xu's e-mail address is xuhaixia_xhx@163.com.

References

1. M. Walessa and M. Datcu, IEEE Trans. Geosci. Rem. Sens. **38,** 2258 (2000).
2. F. T. Ulaby, F. Kouyate, B. Brisco, and T. H. L. Williams, IEEE Trans. Geosci. Rem. Sens. **24,** 235 (1986).
3. W. W. Irving, L. M. Novak, and A. S. Willsky, IEEE Trans. Aero. Electron. Syst. **33,** 1157 (1997).
4. J. Shi and J. Malik, IEEE Trans. Pattern Anal. Mach. Intell. **22,** 888 (2000).
5. S. Yu and J. Shi, in *Proceedings of IEEE Conference on Computer Vision and Pattern Recognition* **2,** 39 (2003).
6. R. Jenssen, T. Eltoft, and J. C. Principe, in *Proceedings of International Joint Conference on Neural Networks* 111 (2004).
7. Z. Wu and R. Leahy, IEEE Trans. Pattern Anal. Mach. Intell. **15,** 1101 (1993).
8. N. Cristianini, J. Shawe-Taylor, and J. Kandola, in *NIPS 2001 Conference Proceedings, Advances in Neural Information Processing Systems* 649 (2001).
9. C. H. Q. Ding, X. He, H. Zha, M. Gu, and H. D. Simon, in *Proceedings of the 2001 IEEE International Conference on Data Mining* 107 (2001).
10. P. Perona and W. Freeman, in *Proceedings of European Conference on Computer Vision* 655 (1998).
11. T. M. Cover and J. A. Thomas, *Elements of Information Theory* (Wiley, New York, 1991) p.18, 19.
12. H. Chen and P. K. Varshney, in *Proceedings of Fusion' 2000* MoD3-9 (2000).
13. M. Holden, D. L. G. Hill, E. R. E. Denton, J. M. Jarosz, T. C. S. Cox, T. Rohlfing, J. Goodey, and D. J. Hawkes, IEEE Trans. Med. Imag. **19,** 94 (2000).
14. R. G. Keys, IEEE Trans. Acous. Speech Signal Process. **29,** 1153 (1981).
15. F. Maes, A. Collignon, D. Vandermeulen, G. Marchal, and P. Suetens, IEEE Trans. Med. Imag. **16,** 187 (1997).
16. H. Chen and P. K. Varshney, IEEE Trans. Med. Imag. **22,** 1111 (2003).